

Positron-lifetime measurements between 300 and 800 K in GaAs and GaP

S. Dannefaer and D. Kerr

Physics Department, University of Winnipeg, Winnipeg, Manitoba, Canada R3B 2E9

(Received 27 October 1993)

Positron-lifetime measurements performed at high temperature have been used to investigate vacancy-like defects in various samples of GaAs and in GaP. A detailed three-state trapping model, which allows for detrapping, is utilized to show that monovacancylike defects trap positrons with a binding energy of close to 0.3 eV, while vacancy clusters constitute traps deep enough such that no detectable detrapping occurs up to 800 K.

I. INTRODUCTION

In a recently published paper¹ (henceforth referred to as Paper I) we demonstrated the feasibility of performing conventional positron lifetime measurements at temperatures up to (at least) 800 K. Positron detrapping was observed to occur in as-grown undoped semi-insulating GaAs and as-grown undoped InSb which permitted the direct determination of absolute specific positron trapping rates and positron binding energies. The data presented in Paper I were simple in the sense that they could be explained entirely on the basis of detrapping from a single trap type, the monovacancy. In this paper we present further high-temperature data on various types of GaAs and also on the wide-gap semiconductor GaP.

In some of these samples, a more complex situation arises because two different types of positron traps coexist requiring an extension of the model considered in Paper I. The two trap types are a trap from which detrapping is observed to occur (shallow trap) and a trap which exhibits no detrapping up to the highest measurement temperature (deep trap). It is demonstrated that the high-temperature measurements make possible the distinction between lifetime components which otherwise would not be separable due to their numerical proximity. Since the detrapping model employed here is central to the interpretation of the results, its development and implications are shown in some detail in the Appendix.

Two discrepancies of long standing exist in the case of positron studies of GaAs. One is related to the value of the bulk lifetime and the other to the question of positron trapping by native vacancies in *p*-type and semi-insulating GaAs. These discrepancies are examined in the final section of the main paper.

II. EXPERIMENT

The experimental conditions were identical to those described in Paper I. Recapitulating briefly, each lifetime spectrum was accumulated to a total of $(6-7) \times 10^6$ counts during 18 h using a lifetime spectrometer with a rather modest time resolution of 250 ps (full width at half maximum). Source corrections were made which were temperature dependent and amounted to a total of 4% of

the entire lifetime spectrum. Analyses were done with a PC version of RESOLUTION (Ref. 2) in which a global fit is obtained of both the resolution function and the annihilation spectrum. The analyses were performed as described in Ref. 3, such that possible systematic errors arising from the usual arbitrary choice of the analysis range were avoided. The samples were heated up to 800 K in a vacuum for several days but showed no sign of surface degradation.

The samples investigated were liquid-encapsulated Czochralski-grown GaAs doped with $3 \times 10^{18}/\text{cm}^3$ Cd (*p* type) or with $3 \times 10^{18}/\text{cm}^3$ Si (*n* type). A low-temperature (850 °C) undoped (but *p* type) liquid-phase electroepitaxially (LPEE) grown material was also investigated. Finally, GaP doped with $5 \times 10^{17}/\text{cm}^3$ S (*n* type) was investigated in order to include a wide-gap semiconductor in addition to the narrow-gap semiconductor InSb (Paper I). Measurements were done going up and down in temperature in order to establish that the changes observed indeed were reversible.

In the next section data will be shown where the lifetime spectra show a transition with temperature from two components to only one component. The necessity for two-component fits was based on the goodness-of-fit values (i.e., assuming only one component gave too high values). When satisfactory goodness-of-fit values (1.00 ± 0.06) could be obtained using only one component, no further decomposition was attempted.

III. RESULTS

In Fig. 1 are shown the results for the liquid-phase epitaxially grown GaAs.⁴ The two resolvable lifetimes τ_1 and τ_2 both decrease above ~ 500 K while I_2 increases towards 100%. The bulk lifetime τ_B^{TM} was calculated according to Eq. (A10) omitting the last term since this term is not present for this sample. These calculated values increase slowly with temperature but are calculable only up to the point where τ_1 can be resolved. The temperature variations of the data resemble very much those from Paper I and are interpreted in the same way, i.e., on the basis of positron detrapping. Using the detrapping model, as described in the Appendix, best fits to the data are shown assuming that no deep traps are present, an assumption which is based on the fact that I_2

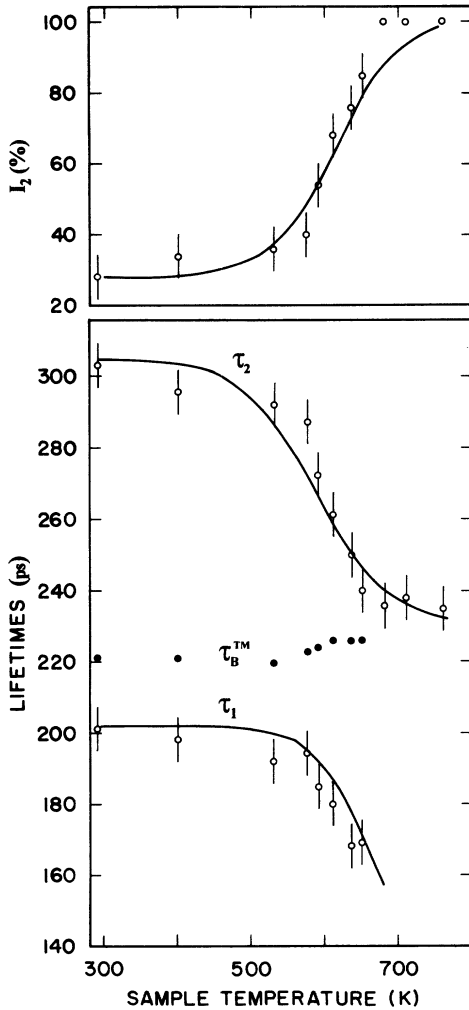


FIG. 1. Positron lifetime data for undoped GaAs (LPEE grown, p type). The curves shown correspond to a binding energy of $E_B=0.32$ eV for a trap with lifetime $\tau_{ST}=304$ ps, $\mu_{ST}=1.0\times 10^{-17}$ cm³/ns, $\tau_B=220+0.01$ ps/K, and $\kappa_{ST}=0.35$ ns⁻¹.

approaches 100%. The curves shown correspond to a positron binding energy of 0.32 eV and absolute specific trapping rate μ_{ST} of 1.0×10^{-17} cm³/ns.

The data for heavily Si-doped GaAs are shown in Fig. 2. They resemble the data in Fig. 1 again indicating detrapping with increasing temperature but also show a persistent, although weak, 340-ps component even at the highest temperature. As described in the Appendix, this is indicative of a deep trap (or rather a trap which shows no perceptible detrapping up to 800 K).

Figure 3 shows the data for Cd-doped GaAs (p type). This sample is different from all the other GaAs samples (including the GaAs sample in Paper I) in several regards. There is essentially no temperature dependence of the lifetime and intensity parameters. The τ_2 value is large (~ 325 ps) as is its intensity (16%), and the bulk lifetime calculated from Eq. (A10) (omitting the last term since only two components could be resolved) is also

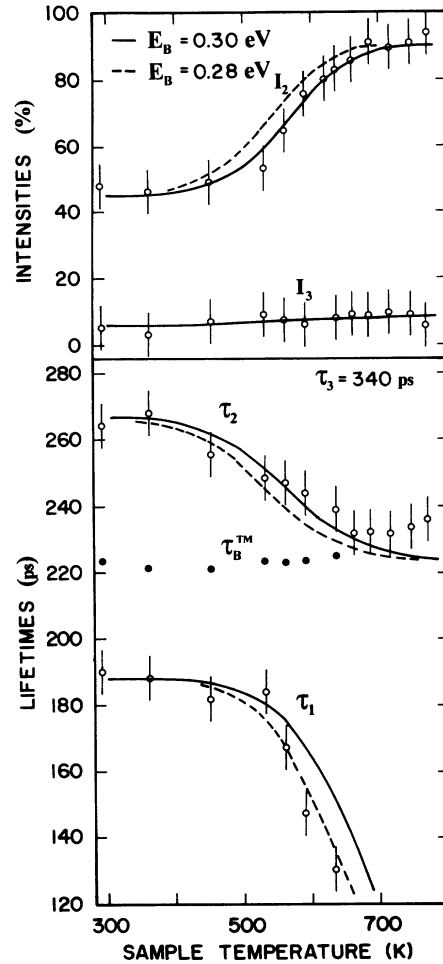


FIG. 2. Positron lifetime data for GaAs:Si (3×10^{18} /cm³, n type). The curves shown are calculated using the following parameters: $\tau_B=220+0.01$ ps/K, $\tau_{ST}=266$ ps, $\tau_{DT}=\tau_3=340$ ps, $\kappa_{ST}=0.7$ ns⁻¹, $\kappa_{DT}=0.14$ ns⁻¹, $\mu_{ST}=\mu_{DT}=1\times 10^{-17}$ cm³/ns. Two different E_B values were assumed in order to illustrate the sensitivity to E_B .

large (~ 235 ps compared to ~ 220 ps) possibly indicating that the assumed one-defect trapping model is not applicable.

The final sample investigated was S-doped GaP (n type), a wide-gap semiconductor. The data shown in Fig. 4(a) are initially puzzling. Although the resolved lifetime parameters (τ_1 , τ_2 , and I_2) appear strongly temperature dependent, their behavior is essentially opposite to that seen in the other samples where a temperature dependence was also observed. An important feature of the data is that τ_2 assumes a large value in the high-temperature region and persists with a sizable intensity even up to 800 K. This is indicative of the presence of a deep trap which should, in fact, be effective over the entire temperature range. As described in the Appendix this trap may be difficult to detect due to the proximity of the positron lifetimes in the deep and shallow traps. Guided by these considerations, the following assump-

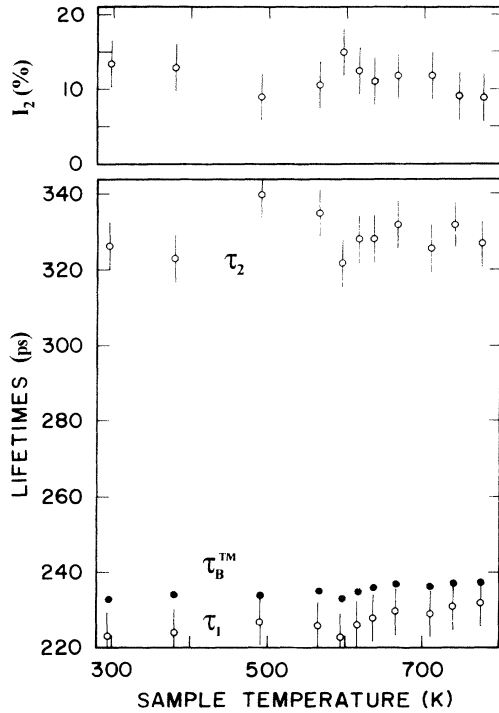


FIG. 3. Positron lifetime data for heavily Cd-doped GaAs ($3 \times 10^{18}/\text{cm}^3$, p type).

tions were made: The ~ 305 -ps lifetime resolved at room temperature [Fig. 4(a)] is actually a composite of two lifetimes, the 334-ps (τ_3) component resolved only at high temperatures and an unresolved lifetime τ_2 . It is straightforward to calculate that this unresolved lifetime has a value of 290 ps in order to be self-consistent with the lifetime and intensities resolved around room temperature.

It became possible, albeit only by fixing the 334-ps component, to resolve an additional lifetime component (τ_2) in the temperature range 550–650 K, producing the results in Fig. 4(b). As a final step, theoretical curves can now be calculated assuming that the τ_2 component arises from a shallow trap whereas τ_3 arises from a deep trap. To produce agreement with the 300-K and the > 700 -K data the trapping rates κ_{ST} and κ_{DT} had to be 0.6 and 0.35 ns^{-1} , respectively. A binding energy close to 0.31 eV yields quite a good fit in the temperature range where decomposition is possible (region II) as well as reproducing the trends in region I where only average values of τ_2 and τ_3 could be found.

Because computational artifacts may give rise to artificial lifetime components, a comment on the decomposition of some of the lifetime spectra into two components is appropriate. First, as noted above, two-component analyses were performed only when demanded by the goodness-of-fit values. Second, the fact that there is a transition with temperature from one- to two-component fits indicates that there is no intrinsic bias toward two-component fits. Finally, the τ_1 , τ_2 , and I_2 data can be explained by the detrapping model which is not inherent to the data analysis.

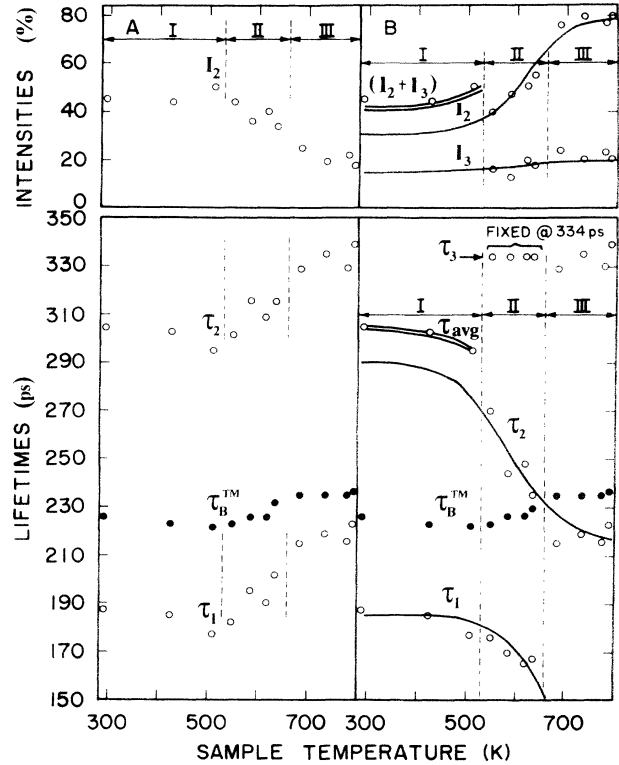


FIG. 4. (a) Results for GaP assuming two lifetime components and τ_B^{TM} values based on these analyses. (b) Three regions are indicated (I, II, III). In regions I and III no further decomposition was possible so data points are identical to those from (a). In region II an additional lifetime could be resolved (τ_2) when τ_3 was fixed to the average value (334 ps) found in the two-term analyses in region III. Note the change in the identification of the lifetimes here as compared with (a). As described in the Appendix, τ_1 eventually becomes too small to be detectable so that in region III the shortest resolvable component is actually τ_2 and the longest is actually τ_3 . Best fit theoretical curves (—) are shown as calculated with: $\tau_{DT} = 334$ ps, $\tau_{ST} = 290$ ps, $\tau_B = 221 + 0.01$ ps/K, $\kappa_{ST} = 0.6$ ns^{-1} , $\kappa_{DT} = 0.35$ ns^{-1} , $\mu_{ST} = \mu_{DT} = 1 \times 10^{-17}$ cm^3/ns , and $E_B = 0.31$ eV. The two double-lined segments of curves in region I correspond to the theoretically predicted average lifetimes (τ_{avg}) and sum of intensities ($I_2 + I_3$) to which the experimental data should be compared in region I. Error bars of data points are omitted for the sake of clarity in this figure.

IV. DISCUSSION

In order to provide an overall view, the results for all samples, including those in Paper I, are collected in Table I. It appears from Table I that defects which result in positron lifetimes in the range 270–305 ps have positron binding energies close to 0.3 eV, while defects with lifetimes between 330 and 360 ps have binding energies so large that detrapping is not observed at 800 K, which indicates a lower limit of ~ 0.6 eV. It is not possible at this point to establish if there are differences in E_B within each group of lifetimes because the value of the absolute specific trapping rate is not known accurately enough. In

TABLE I. Collection of results for all samples investigated up to 800 K.

| Sample | Temperature range (K) | Bulk lifetime at 300 K (ps) | Defect lifetimes (ps) | μ ($10^{-17}\text{cm}^3/\text{ns}$) | E_B (eV) | Comments |
|--|-----------------------|-----------------------------|-----------------------|---|------------|--|
| SI-GaAs ^a | 30–775 | 223 | 290 | 0.9–1.3 | 0.28–0.30 | |
| LPEE-GaAs (undoped, <i>p</i> type) | 300–760 | 220 | 305 | 1–2 | 0.32–0.35 | |
| GaAs:Cd ($3 \times 10^{18}/\text{cm}^3$, <i>p</i> type) | 300–780 | 233 | 330 | | > 0.6 | No observable detrapping |
| GaAs:Si ($3 \times 10^{18}/\text{cm}^3$, <i>n</i> type) | 300–780 | 222 | 270 | 1–2 | 0.28–0.30 | |
| GaP:S ($5 \times 10^{17}/\text{cm}^3$, <i>n</i> type) | 300–800 | 222 | 350 | | > 0.6 | |
| | | | 290 | 1–2 | ~ 0.31 | |
| | | | 335 | | > 0.6 | |
| InSb ^a | 30–810 | 266 | 305 | 1.2–2.0 | 0.32–0.6 | E_B increases above ~ 500 K to 0.6 eV close to the melting point |

^aFrom Ref. 1.

fact, only for the SI-GaAs samples were the data sufficiently accurate to establish a narrow range. Nevertheless, the proximity of all E_B values to 0.3 eV strongly suggests that the lifetimes in the 270–305-ps range all arise essentially from the same type of defects, and these defects are most likely monovacancies. The spread in the monovacancylike lifetimes from sample to sample can be explained by assuming that the grown-in vacancies are associated with impurities or other structural defects. The evidence for this comes from the earlier observed thermal stability of grown-in defects up to at least 600 °C.⁵ In contrast to our earlier interpretations it appears that the spread in monovacancy lifetimes can be larger than first anticipated.

Recent theoretical calculations⁶ of the positron binding energy are generally in good agreement with the experimental ones, except in the case of GaP, where very small theoretical binding energies are found (0.08 eV for V_{Ga} and *no* trapping for V_{P}). In the cases of defects which have the larger positron binding energies the lifetime would suggest defect clusters of at least two vacancies, and theoretical calculation indeed indicates that such defects would have binding energies ~ 1 eV, except, again, in the case of GaP (0.27 eV for $V_{\text{Ga}}V_{\text{P}}$).

Apart from the work presented in Ref. 1 there are only a few reports on high-temperature measurements on compound semiconductors. In one paper on GaAs, Soininen *et al.*⁷ used slow positron diffusion data, i.e., positron data not based on lifetime measurements but rather on the less specific Doppler broadening data, to deduce that up to 900 K no apparent influence from defects could be found. This in turn could be taken as evidence that in *p* type GaAs no trapping by vacancies takes place (this will be discussed further in the next section). Although this may be construed as incompatible with the present data since detrapping of trapped positrons would increase the diffusivity, we do point out that the *fraction* of positron trapped, to which the Doppler signal is proportional, is quite small, only about ~ 20% [defined as $\kappa/(\kappa + \lambda_B)$]. We do not believe that a change in trapped

fraction from ~ 20% to ~ 0% at high temperatures could have been observable in these diffusion experiments.

Another high-temperature experiment was recently reported by Krause-Rehberg *et al.*,⁸ in this case using positron lifetime measurements, on GaP up to 550 K. In this lightly Si-doped material they found a decrease in I_2 from 65% to 50% between 350 and 450 K, which was attributed to a shift from V_{P}^- to V_{P}^0 resulting from a decrease in the position of the Fermi level. Since our GaP is more heavily doped (with S) it is hardly surprising that this is not observed in our case. We do, however, observe a decrease in I_2 above 550 K [see Fig. 4(a)] but as argued in the preceding section, this stems from a computational artifact from the two-component analysis. Nevertheless, because of this suggestion that negatively charged V_{P} might be traps for the positrons, low-temperature measurements between 30 and 300 K were performed, but no indication for negatively charged vacancies could be found as evidenced by the lack of an increased trapping at low temperature. Thus we have used an absolute trapping rate pertinent to neutral vacancies in the calculations of the curves shown in Fig. 4(b).

V. BULK LIFETIMES AND TRAPPING IN *p*-TYPE AND SEMI-INSULATING GaAs

We now turn our attention to the discrepancies which exist among bulk lifetimes reported for GaAs and the observation of positron trapping at vacancies in *p* type and semi-insulating GaAs.

The bulk lifetime is expected to exhibit a temperature dependence due to the thermal expansion of the lattice and may be linked to the volume expansion by means of the equation

$$\tau_B(T) = \tau_B^0 [1 + 3\beta\Delta L(T)/L_0], \quad (1)$$

where τ_B^0 is the value of τ_B at temperature $T=0$ K, $\Delta L(T)/L_0$ is the relative linear expansion, and β is a scaling constant. It is convenient to write Eq. (1) as

$$\frac{\Delta\tau}{\tau_B^0} = \frac{\tau_B(T) - \tau_B^0}{\tau_B^0} = 3\beta\Delta L(T)/L_0, \quad (2)$$

with

$$\Delta L(T)/L_0 = \int_0^T \alpha(T) dT. \quad (3)$$

Here $\alpha(T)$ is the thermal expansion coefficient.

In Fig. 5 volume expansion values $3\Delta L(T)/L_0$ [obtained from data on $\alpha(T)$ in Ref. 9] are plotted as a function of temperature for both GaAs and InSb and we note that below ~ 200 K there is a clear deviation from linearity. Values of $\Delta\tau/\tau_B^0$ for GaAs and InSb (from Paper I) are also shown in Fig. 5, and despite the scatter in the data points, the trend suggested by the volume expansion is reproduced. Thus, there is some support for the identification of τ_B^{TM} as the actual bulk lifetime. However, it is important to realize that although the bulk lifetime should reflect the thermal expansion behavior, observing this is by itself not sufficient to unequivocally identify an observed lifetime as the bulk lifetime. This can clearly be seen when calculating the typical case of trapping at a single defect type with a constant trapping rate (and no detrapping) from which one finds that the average lifetime (given by $I_1\tau_1 + I_2\tau_2$) has a temperature dependence very closely approximating that of the bulk lifetime.

In a recent study of GaAs, Saarinen, Hautojärvi, and Lanki¹⁰ resolved only a single lifetime component in *p* type material which apparently increased linearly in the 85–600-K temperature range (their lowest measurement temperature being about the point at which the non-linearity might have begun to be evident). The single resolvable component was interpreted as the bulk lifetime

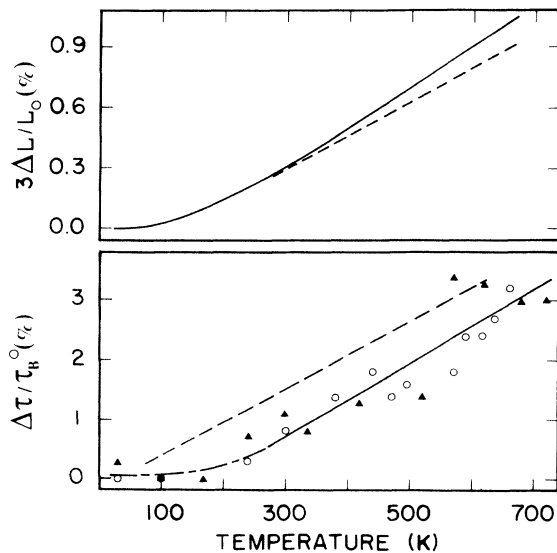


FIG. 5. In the upper panel is shown the volume expansion as a function of temperature for GaAs (solid line) and InSb (broken line). In the lower panel the percentage increase in bulk lifetime is shown for GaAs (●) and InSb (△). The broken line shows the results obtained by Saarinen, Hautojärvi, and Lanki (Ref. 10) for GaAs.

whose 231-ps value at 300 K (the same value as reported by them in an earlier study) is mildly discrepant with our current and earlier reported value of about 220 ps.

These discrepancies together with the above discussion, raise the question whether the single lifetime resolved by Saarinen Hautojärvi, and Lanki,¹⁰ although behaving like a bulk lifetime, is actually an average lifetime.

If so, the value would be higher than the bulk lifetime and their values are indeed higher than ours by ~ 10 ps. Further, the calculation of average lifetimes from our resolved lifetimes and intensities yields values (235 and 229 ps for LPEE GaA and Si-doped GaAs, respectively) close to their 231-ps value.

Notwithstanding the above comments, a discrepancy of only 10 ps may be purely experimental in origin. Saarinen, Hautojärvi, and Lanki¹⁰ routinely accumulate $(1-2)\times 10^6$ counts per spectrum in contrast to our $(6-8)\times 10^6$ counts; time resolution functions differ and they use one Gaussian to approximate its shape whereas we use two Gaussians, and finally, source corrections differ significantly. Unfortunately, theoretical calculations are unable to predict with an accuracy any better than the existing difference.

A much more important issue is the general claim by Saarinen, Hautojärvi, and Lanki¹⁰ and by the same group in earlier works that only in *n*-type GaAs does positron trapping by vacancies occur. In direct contrast, in this as well as earlier investigations we have found clear evidence of trapping in *p* type and semi-insulating GaAs. We are forced to conclude that positron trapping can occur in these materials but that the degree to which this happens may be strongly sample dependent. It is important to point out that charge considerations are not as straightforward as they might appear to be, since the vacancies in GaAs are undoubtedly trapped by impurities or other structural defects (as deduced from the fact that the defects are stable up to at least 600 °C) which renders predictions of charged states very uncertain.

VI. CONCLUSION

We have demonstrated that conventional positron lifetime spectroscopy can be extended to at least 800 K of measuring temperature making possible the experimental determination of binding energies for monovacancylike defects.

Based on a detrapping model it has been possible to obtain positron binding energies in GaAs, InSb, and GaP. Defects of monovacancy nature (270–305 ps) all yield a positron binding energy of ~ 0.3 eV and absolute specific trapping rates of $(1-2)\times 10^{-17}$ cm³/ns. Defects resulting in larger lifetimes (330–350 ps) did not exhibit detrapping up to 800 K indicating a binding energy in excess of 0.6 eV. These defects are probably vacancy clusters. Theoretical calculations are generally in good agreement with experiments except in the case of the wide-gap semiconductor GaP. Finally, we have addressed some long-standing problems regarding positron data on GaAs, arguing that their origins may be of a superficial nature.

ACKNOWLEDGMENTS

We are indebted to Dr. P. Mascher who conducted the measurements and to Dr. T. Bretagnon who implemented the detrapping model on the computer. This work was supported by the Natural Sciences and Engineering Research Council of Canada.

APPENDIX

The mathematical framework for a defect situation corresponding to one defect type from which detrapping plays a role plus another defect type from which no detrapping occurs was worked out by Pagh *et al.*¹¹

Figure 6 depicts the above envisaged situation. Positrons are (as usual) assumed initially only to occupy the bulk state, in which they have an annihilation rate of λ_B ($\equiv 1/\tau_B$). From this state positrons can be trapped by the deep trap with a rate of κ_{DT} , from which they annihilate with the rate of λ_{DT} . The trapping rate due to the shallow traps is κ_{ST} but detrapping is also occurring from this defect with a temperature dependent rate of δ_{ST} . Annihilations from the shallow trap occur with the rate λ_{ST} . The trapping rates are given by

$$\begin{aligned}\kappa_{DT} &= \mu_{DT} C_{DT}, \\ \kappa_{ST} &= \mu_{ST} C_{ST}.\end{aligned}\quad (A1)$$

C_{DT} and C_{ST} are the defect concentrations of the two defect types. Since absolute concentrations are commonly used in semiconductor physics the absolute specific trapping rates μ_{DT} and μ_{ST} are here expressed in the convenient units of (cm^3/ns). (Sometimes the specific positron trapping rate ν is used, which equals μ times the atomic density of the material in question.)

The detrapping rate is given by¹²

$$\delta_{ST} = \mu_{ST} \left[\frac{m^* k_B T}{2\pi\hbar^2} \right]^{3/2} e^{-E_B/k_B T}.\quad (A2)$$

E_B is the positron binding energy and m^* is the effective

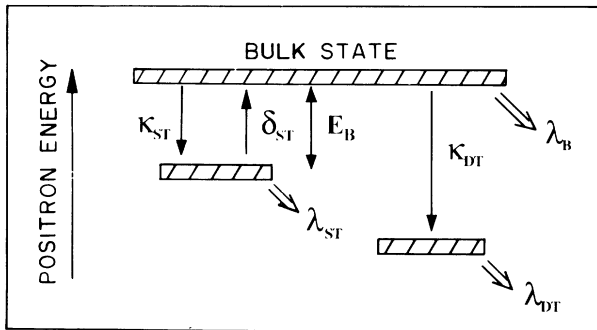


FIG. 6. Schematic diagram representing the positron trapping model involving a trap (ST) which exhibits detrapping and another trap (DT) which exhibits no detrapping. The annihilation rates from the bulk (λ_B), from the shallow trap (λ_{ST}), and from the deep trap (λ_{DT}) are indicated together with the trapping rates (κ_{ST} and κ_{DT}) and the detrapping rate δ_{ST} .

mass which, for positrons, is close to the free mass. We will assume $m^* = m_0$ for positrons in accordance with experimental findings for Ge,¹³ but deviating somewhat from theoretical estimates [$m^* = (1.3-1.6) \times m_0$] by Soininen *et al.*⁷ From the coupled first-order differential equations expressing the time dependencies of the populations in each of the three states shown in Fig. 6, Pagh *et al.*¹¹ find expressions for the experimentally determinable lifetime components τ_1 , τ_2 , and τ_3 ($\tau_1 < \tau_2 < \tau_3$) and their corresponding intensities I_1 , I_2 , and I_3 according to

$$1/\tau_1 \equiv \lambda_1 = (\lambda_B + \kappa_{ST} + \kappa_{DT} + \lambda_{ST} + \delta_{ST} + d),\quad (A3)$$

$$1/\tau_2 \equiv \lambda_2 = \lambda_1 - d,\quad (A4)$$

$$1/\tau_3 \equiv \lambda_3 = \lambda_{DT},\quad (A5)$$

$$I_2 = \left[\lambda_{ST} \kappa_{ST} + (\lambda_{ST} + \delta_{ST} - \lambda_2) \left[\lambda_B - \frac{\lambda_{DT} \kappa_{DT}}{\lambda_2 - \lambda_{DT}} \right] \right] / d \lambda_2,\quad (A6)$$

$$I_3 = \kappa_{DT} \frac{\lambda_{ST} + \delta_{ST} - \lambda_{DT}}{(\lambda_1 - \lambda_{DT})(\lambda_2 - \lambda_{DT})},\quad (A7)$$

$$I_1 = 1 - I_2 - I_3.\quad (A8)$$

In the above expressions the parameter d is

$$d = [(\lambda_B + \kappa_{ST} + \kappa_{DT} - \lambda_{ST} - \delta_{ST})^2 + 4\kappa_{ST} \delta_{ST}]^{1/2}.\quad (A9)$$

Thus the experimentally determined rates (λ_1 , λ_2 , and λ_3) do not necessarily correspond to the annihilation rates (λ_B , λ_{ST} , and λ_{DT}) from the three positron states and the expressions are greatly complicated by δ_{ST} . Despite the complexity of these expressions, it is simple to show that the bulk lifetime is related to the lifetime spectrum parameters according to

$$1/\tau_B \equiv \lambda_B = I_1 \lambda_1 + I_2 \lambda_2 + I_3 \lambda_3.\quad (A10)$$

In fact, this equation holds true regardless of the trapping situation as long as all positrons initially occupy the bulk state.

The bulk lifetime τ_B is the lifetime that would be observed in a sample containing no positron traps. Its value is material dependent and it should increase slowly with temperature as a reflection primarily of lattice expansion. When trapping does occur, then the experimentally observed parameters may be used to calculate the bulk lifetime with Eq. (A10). Values thus obtained are denoted τ_B^{TM} in the main text to indicate that they have been calculated according to the trapping model. A consistency check is therefore provided in the sense that, if the assumed trapping model is valid, the τ_B^{TM} values should compare well with established values and vary as expected with temperature.

In the case of $\delta_{ST} = 0$ (referred to as the simple trapping model), very significant simplifications result. One obtains the results

$$\begin{aligned}\lambda_1 &= \lambda_B + \kappa_{ST} + \kappa_{DT}, \\ \lambda_2 &= \lambda_{ST}, \\ \lambda_3 &= \lambda_{DT}\end{aligned}\quad (A11)$$

[as in Eq. (A5)]. The intensities are now given by the simple expressions:

$$\begin{aligned} I_2 &= \kappa_{ST}/(\lambda_1 - \lambda_{ST}), \\ I_3 &= \kappa_{DT}/(\lambda_1 - \lambda_{DT}), \\ I_1 &= 1 - I_2 - I_3. \end{aligned} \quad (\text{A12})$$

In the case of $\delta_{ST} \rightarrow \infty$, simple expressions are again obtained:

$$\begin{aligned} \tau_1 &= 0, \\ \lambda_2 &= \lambda_B + \kappa_{DT}, \\ \lambda_3 &= \lambda_{DT}, \\ I_1 &= 0, \\ I_3 &= \kappa_{DT}/(\lambda_2 - \lambda_{DT}), \\ I_2 &= 1 - I_3. \end{aligned} \quad (\text{A13})$$

Note, that in this case the τ_1 component has disappeared, and that only the deep trap plays a role.

We will illustrate the use of Eqs. (A2)–(A9) to calculate (τ_i, I_i) values as a function of temperature. Necessary input parameters are all the parameter values shown

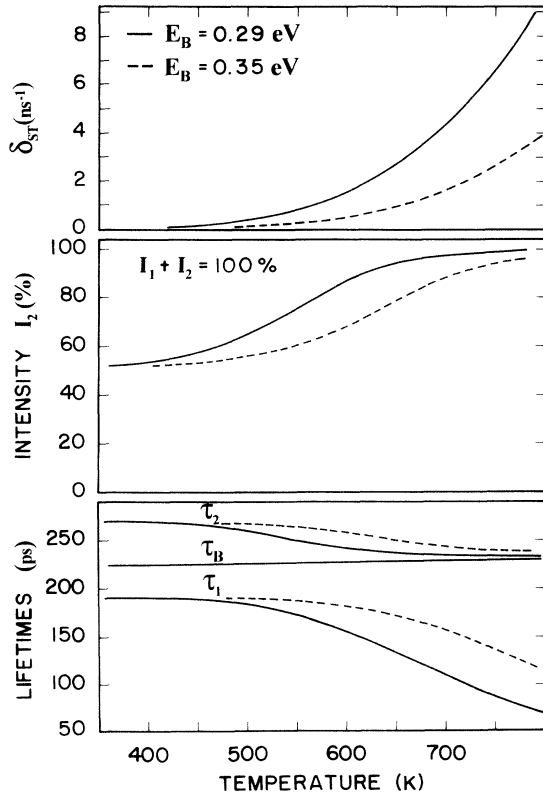


FIG. 7. Calculated observable lifetimes values τ_1 and τ_2 and intensity I_2 of the τ_2 component in the case of no deep trap using the following parameters: $\tau_B = 220 + 0.01$ ps/K, $\tau_{ST} = 270$ ps, $\kappa_{ST} = 0.8$ ns⁻¹, $\mu_{ST} = 1 \times 10^{-17}$ cm³/ns. Detrapping rates δ_{ST} are shown in the upper panel. Calculations were done for the two binding energies indicated.

in Fig. 6. In the first example we will consider the case of no deep traps, i.e., $\kappa_{DT} = 0$, and choose the values of the remaining parameters pertinent to the case of GaAs as described in Paper I. All parameters in the above list are assumed temperature independent, except for $1/\lambda_B$ which is allowed to vary slightly with temperature according to 0.01 ps/K, which approximates the temperature dependence as discussed in Sec. V. In Fig. 7 results are shown for various E_B values. As expected, τ_1 decreases markedly when temperature (and hence δ_{ST}) increases; τ_2 decreases from the intrinsic lifetime value of the shallow trap (τ_{ST}) towards τ_B when δ becomes large, and I_2 approaches 100%. Fairly small values of τ_1 (and $I_1 = 1 - I_2$) are quickly reached, so that experimentally this component is “lost.” In the experiments described in Paper I, as well as here, the lowest detectable value of τ_1 was ~ 120 ps due to the fairly broad resolution of 250 ps. Below this value of τ_1 the only resolvable component will then have values close to τ_B , albeit still slightly larger than τ_B . It is furthermore noteworthy that the two lifetimes τ_1 and τ_2 stay well separated so that mixing of the components does not occur.

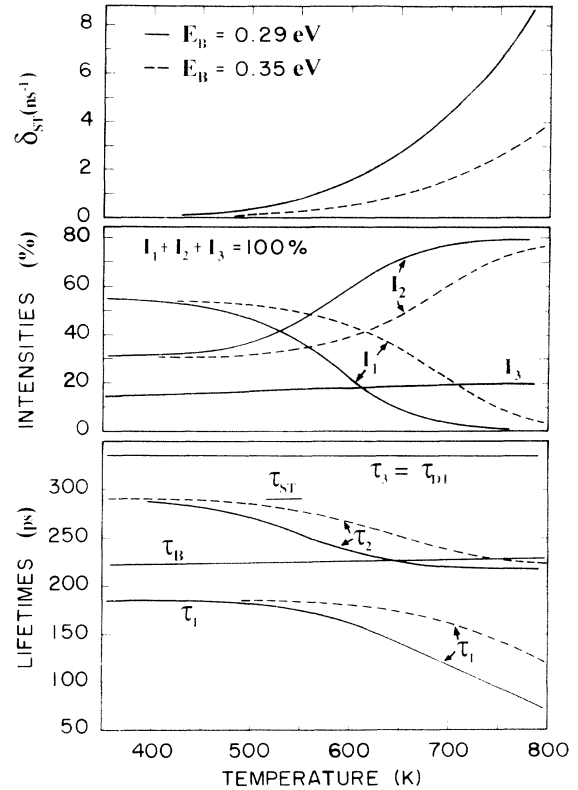


FIG. 8. Calculated observable lifetime values τ_1 , τ_2 , and τ_3 with corresponding intensities I_1 , I_2 , and I_3 according to the following input parameters: $\tau_B = 220 + 0.01$ ps/K. Shallow trap lifetime $\tau_{ST} = 290$ ps with trapping rate 0.6 ns⁻¹. Deep trap lifetime $\tau_{DT} = 335$ ps with trapping rate 0.35 ns⁻¹. Absolute specific trapping rates $\mu_{ST} = \mu_{DT} = 1 \times 10^{-17}$ cm³/ns. Detrapping rates are shown in the upper panel. Calculations were done for two binding energies for which the curves for I_3 are identical on the scale of the drawing.

Adding another defect type which introduces a deep trap with a positron lifetime of τ_{DT} results in a situation as depicted in Fig. 8. The parameter values chosen are those pertinent to GaP. The comments made regarding Fig. 7 apply also to Fig. 8 although with the difference that τ_2 approaches not τ_B , but rather a smaller value determined by Eqs. (A13), because of the persistent influence from the deep traps. Consequently I_2 does not approach 100%.

There is, however, a point to be made again from an experimental perspective. The two lifetimes τ_{ST} and τ_{DT} were chosen quite close together, in fact so close that when at lower temperatures where *both* the experimentally resolvable lifetimes τ_2 and τ_3 equal these lifetimes, respectively, they would in fact not be resolvable. Instead a weighted average would be found according to

$$\tau_{avg} = (I_2\tau_2 + I_3\tau_3) / (I_2 + I_3), \quad (A14)$$

so that the lifetime spectrum would only contain two components, τ_{avg} and τ_1 . Now, as the temperature is in-

creased the numerical separation between the decreasing τ_2 and the constant τ_3 values becomes larger, so at some point it may become possible to resolve all three lifetime components. This situation persists until τ_1 has become too low to be detectable, and then again only two components become resolvable, which now physically correspond to $\tau_3 = \tau_{DT}$ and $\tau_2 = (\lambda_B + \kappa_{DT})^{-1}$, according to Eq. (A13).

In view of the above, we would like to point out the inherent danger in assuming that certain lifetimes are averaged together when detrapping occurs. Because the numerical values of the lifetimes change significantly with temperature it is generally unpredictable just which averaging the least squares computer fitting procedure of the raw spectra will decide on.

From Figs. 7 and 8 it can be observed that from the experimental point of view, the temperature variation of I_2 is the most sensitive to E_B in the intermediate temperature change. At the highest temperatures, however, the τ_1 component exhibits the largest sensitivity, but to take advantage of this, a lifetime spectrometer with high stability and very good time resolution is required.

¹S. Dannefaer and D. Kerr, Phys. Rev. B **48**, 9142 (1993).

²P. Kirkegaard, M. Eldrup, M. Mogensen, and N. J. Petersen, Comput. Phys. Commun. **23**, 307 (1981).

³T. Bretagnon, K. Abdurahman, D. Kerr, and S. Dannefaer, Mater. Sci. Forum **105-110**, 1841 (1992).

⁴Results for this and other samples were reported earlier, in P. Mascher, S. Dannefaer, and D. Kerr, in *Defect Control in Semiconductors*, edited by K. Sumino (Elsevier Science, Amsterdam, 1990), p. 777. However, the interpretation of these results was erroneous because of an incorrect data analysis in which the defect lifetime was fixed, i.e., not allowed to vary with temperature, and no account was taken of the temperature-dependent source correction.

⁵S. Dannefaer, P. Mascher, and D. Kerr, J. Phys. Condens. Matter **1**, 3213 (1989).

⁶M. J. Puska, S. Mäkinen, M. Manninen, and R. M. Nieminen,

Phys. Rev. B **39**, 7666 (1989).

⁷E. Soininen, J. Mäkinen, D. Beyer, and P. Hautojärvi, Phys. Rev. B **46**, 13 104 (1992).

⁸R. Krause-Rehberg, A. Polity, W. Siegel, and G. Kühnel, Semicond. Sci. Technol. **8**, 290 (1993).

⁹S. I. Novikova, in *Semiconductors and Semimetals*, edited by R. K. Willardson and A. C. Beer (Academic, New York, 1966), Vol. 2.

¹⁰K. Saarinen, P. Hautojärvi, and P. Lanki, Phys. Rev. B **44**, 10 585 (1991).

¹¹B. Pagh, H. E. Hansen, B. Nielsen, G. Trumphy, and K. Petersen, Appl. Phys. A **33**, 255 (1984).

¹²M. Manninen and R. M. Nieminen, Appl. Phys. A **26**, 93 (1981).

¹³M. A. Shulman, G. M. Beardsley, and S. Berko, Appl. Phys. **5**, 367 (1975).